Desalination and Water Treatment
www.deswater.com
doi: 10.5004/dwt.2021.27676

239 (2021) 217–227
November

Polyethersulfone coated Ag-SiO_2 nanoparticles: a multifunctional and ultrafiltration membrane with improved performance

Shahid Ali Khan[a], Zulfiqar Ahmad Rehan[d,*], Salman S. Alharthi[e], Eid H. Alosaimi[f], Lassaad Gzara[g], M.S. El-Shahawi[c], Khalid A. Alamry[c], Kalsoom Akhtar[c], Esraa M. Bakhsh[c], Abdullah M. Asiri[b,c], Sher Bahadar Khan[b,c,*], Enrico Drioli[h]

[a]*Department of Chemistry, University of Swabi, Anbar-23561, Khyber Pakhtunkhwa, Pakistan, email: shahidsawal007@gmail.com (S.A. Khan)*
[b]*Center of Excellence for Advanced Materials Research (CEAMR), King Abdulaziz University, P.O. Box: 80203, Jeddah, Saudi Arabia 21589, emails: sbkhan@kau.edu.sa (S.B. Khan), aasiri2@kau.edu.sa (A.M. Asiri)*
[c]*Department of Chemistry, King Abdulaziz University, P.O. Box: 80203, Jeddah, Saudi Arabia 21589, emails: malsaeed@kau.edu.sa (M.S. El-Shahawi), k_alamry@yahoo.com (K.A. Alamry), kaskhan@kau.edu.sa (K. Akhtar), ibakhsh@kau.edu.sa (E.M. Bakhsh)*
[d]*Department of Materials, National Textile University Faisalabad Pakistan, email: zarehan@ntu.edu.pk*
[e]*Department of Chemistry, College of Science, Taif University, P.O. Box: 11099, Taif 21944, Saudi Arabia, email: salmanalharthi@hotmail.com*
[f]*Department of Chemistry, College of Science, University of Bisha, P.O. Box: 511, Bisha 61922, Saudi Arabia, email: eid_142@hotmail.com*
[g]*Center of Excellence in Desalination Technology, King Abdulaziz University, P.O. Box: 80200, Jeddah 21589, Saudi Arabia, email: lassaadgzara@gmail.com*
[h]*Institute on Membrane Technology (ITM-CNR), c/o University of Calabria, Via P. Bucci 17/C, 87030 Rende, (CS), Italy, email: e.drioli@itm.cnr.it*

Received 25 May 2021; Accepted 2 August 2021

ABSTRACT

Silver-silica (Ag-SiO_2) embedded in polyethersulfone (PES) composite membranes were prepared by adding different ratios of Ag-SiO_2 in PES and designated as PES-Ag-SiO_2-01 ~ PES-Ag-SiO_2-05. The synthesized hybrid membranes were investigated to check the influence of Ag-SiO_2 on the morphology, hydrophilicity, porosity, mechanical properties, water permeability, bovine serum albumin (BSA) separation, nitrophenol adsorption and antibacterial characteristics of the hybrid membranes. The inclusion of Ag-SiO_2 enhanced the porosity of PES hybrid membranes (79% ~ 84.7%) and as result, the hybrid membranes exhibited lower mechanical properties comparative to PES membranes. However, the hydrophilicity of the PES hybrid membranes was enhanced by adding Ag-SiO_2 nanoparticles causing a gradual decrease in contact angle (73.4° to 58.8°). The hybrid membranes displayed higher water permeability and nitrophenol adsorption as compared to pure PES and furthermore these properties were enhanced by increasing Ag-SiO_2 content in the PES hybrid membrane. The hybrid membrane with higher contents of Ag-SiO_2 showed a water flux of 127.7 L/hm^2 which is much greater than pure PES membrane (73.30 L/hm^2). In addition, the PES hybrid membrane exhibited a strong BSA rejection and PES-Ag-SiO_2-04 showed a maximum BSA rejection (91%). The incorporation of Ag-SiO_2 nanoparticles improved the antimicrobial activity of the membranes which strongly depend on the contents of nanoparticles.

Keywords: Polyethersulfone; Ag-SiO_2; Hybrid membranes; Ultrafiltration; Water permeability; Bovine serum albumin rejection; Nitrophenol adsorption; Antibacterial properties

* Corresponding authors.

1. Introduction

Several methods have been developed for water purification [1–3]. Microfiltration techniques were introduced by the water supply organization. These techniques are cost-effective and act as a substitute to program filtration process for the reduction of microbial load in the water resources and are used as a better option for reverse osmosis as a pre-treatment option for demineralization [4]. The colloidal and microbes such as bacteria and viruses (up to 50 nm particle size) can be removed through microfiltration. However, the removal efficiency of the particles such as bacteria, viruses, germs and colloidal are further enhanced to 3 nm with the advent of ultrafiltration technique. The ease and reliability of membrane technologies are frequently used in water filtration systems [5]. However, membrane fouling is one of the key factors, which effect and deteriorates membrane performance [6,7]. Membrane fouling is defined as the accumulation or deposition of particles, colloids, germs, macromolecules, salts, etc. on the surface of the membrane or interstices inside the membrane pores or the wall of the pores are called membrane fouling [8]. There are three types of membrane fouling; bio-fouling, inorganic-fouling and organic-fouling [9], bio-fouling is the most important in deteriorating the membrane structure and performance among others [10,11]. Bio-fouling is problematic to remove due to the deposition of organic constituents inside the pore size and re-growth of microorganisms even at low nutrients concentration which causes contamination of membranes and reduces membrane lifetime [10–12]. However, research has been continued in academics and industries to improve membrane anti-biofouling properties. Polyethersulfone (PES) membranes have largely been utilized for the removal of small particles, bacteria, viruses, fungi, etc. from water. PES has hydrophilic nature and thus wet out quickly. These quick wettability characteristics of PES, results in fast and efficient filtration with the incorporation of the particles [13]. Besides, PES is one of the most attractive polymers in terms of high mechano-chemical properties and thermal, stability and high tolerance towards oxidation [12,14,15]. Membrane anti-fouling characteristic is enhanced by adding a biocidal material [7,16].

Nanomaterials have been frequently used as a biocidal material in the manufacturing of membranes, allowing permeability control and fouling resistance in various structures and relevant functionalities [17]. Different nanomaterials such TiO_2, ZnO, CNT, Al_2O_3, etc. have been used to increase the hydrophilicity of the polymer membrane surface and have resulted in desired outputs of improved permeability, inhibition of microbes, etc. However, silica has a special impact on the perfection and hydrophilicity of the polymer membrane surface because silica has been reported to be a more appropriate inorganic filler for these applications. Thus Ag-SiO_2 NPs (nanoparticles) will greatly enhance the hydrophilicity, filtration characteristics, adsorption properties and antimicrobial characteristics of the membrane surface.

Silver has been used for the treatment of several diseases and infections. It was reported that silver was used by the earliest people to improve the ecosystem [17]. Silver has been confirmed to be effective against severe chronic osteomyelitis, tract infections, and urinary, central venous catheter and burn infections [18]. Recently, it is documented that silver nanoparticles are used as antibacterial agents against *Staphylococcus epidermidis*, methicillin-resistant *Staphylococcus epidermidis* (MRSE), *Escherichia coli*, and methicillin-resistant *Staphylococcus aureus* (MRSA) [19,20]. Silver nanoparticles are also used for the inhibition of *E. coli* [19]. For a long time, silver nanoparticles and silver ions comprise broad spectrum anti-bacterial characteristics, bactericidal and strong inhibitory effect as well as low toxicity to mammalian cells [7].

4-Nitrophenol (4-NP) is one of the most intractable substances present in industrial wastewaters, which have a carcinogenic character and high toxicity [21]. A lot of methods have been developed for its removal, including adsorption, microbial degradation, photo-catalytic degradation electrochemical treatment, catalytic reduction and so on [22,23].

In the present study, we synthesized PES embedded Ag-SiO_2 nanocomposites and characterized by various spectroscopic techniques. Mechanical, porosity, hydrophilicity, water permeability, bovine serum albumin (BSA) rejection, nitrophenol adsorption and antibacterial performance were evaluated.

2. Experimental section

2.1. Materials

PES of Mw = 66 kDa in powder form (d = 1.37 g/cm^3) was purchased from Sigma-Aldrich (Germany). Before use, PES powder was dried in a vacuum oven at 105°C. 1-Methyl-2-pyrrolidone (NMP, 99.5%) and BSA were obtained from Sigma-Aldrich Co. Ultrapure water (PURELAB Elga, UK) was used for the preparation of the solutions and also for coagulation bath. BSA solution (500 mg/L, pH 7.0) was prepared using 0.2 M phosphate buffer solution. Cetyltrimethylammonium bromide (CTAB), silver nitrate, tetraethyl orthosilicate (TEOS), ethanol and NH_4OH were purchased from Sigma-Aldrich. Unless specified, all of the reagents were used as received without further purification.

2.2. Synthesis of Ag-SiO_2

Ag-SiO_2 was prepared by employing sol–gel method [23]. Firstly 0.2 g silver nitrate ($AgNO_3$) and 0.6 g of surfactant CTAB were dissolved in 20 mL deionized H_2O and then 60 mL C_2H_5OH was added to this mixture and kept on stirring by using the magnetic bar. After that added 6 mL NH_4OH. To the same solution 0.4 g TEOS was added. The resultant solution was heated overnight at 50°C and named as Ag-SiO_2 solution.

2.3. Synthesis of PES-Ag-SiO_2 hybrid membranes

To prepare the PES-Ag-SiO_2 hybrid membranes, different amount of Ag-SiO_2 solution was firstly evaporated on a hotplate to remove water and then dissolved in NMP followed by sonication at 40°C until the complete dispersion of nanoparticles followed by the addition of PES. The stirring was carried out at 5.0 Hz (300 rpm) and 60°C. After complete dissolution, air bubbles were removed

from the solution by degassing and the solution. The dope solution was sprinkled on a glass substrate and the membrane was cast with a casting knife of thickness 250 μm by an automatic film applicator machine from Ericsson GmbH with a casting speed of 30 mm/s. The membranes were instantly immersed in an ultrapure water coagulation bath at 25°C to persuade phase separation. All the residual solvents were leached out by putting the membranes in ultrapure water for 24 h and then dried at room temperature. Table 1 shows the composition of the PES-Ag-SiO_2 nanocomposite membrane prepared in the study.

2.4. Membrane characterization

Surface morphologies and cross-section of the PES-Ag-SiO_2 membranes were examined by field emission scanning electron microscopy (FESEM; FEI, Quanta 450 FEG). Membrane samples were attached to the grid using copper tape and sputtered with gold by means of a sputter coater (Quorum Q150R ES, Quorum Technologies Ltd., Ashford, Kent, England). EDX study of membranes was performed by energy-dispersive X-ray spectroscopy (EDAX Inc., AMETEK, USA). The voltage was set at 20 kV for cross-section and surface images. The freeze-fracture technique was applied by immersing the membrane in liquid nitrogen so that cross-sectional SEM images of nanocomposite membranes can be obtained.

The contact angle measurements were carried out with ATTENSION Theta Tensiometer [25]. A sessile drop method was used to determine the membrane contact angle. For each sample, three measurements were performed in different places and then the average values were reported.

The mechanical properties of the nanocomposite membranes were characterized using an Instron Tensile Test machine. All the specimens were prepared according to standard shape before testing. In particular specimens for the membrane were stretched unidirectional at a 5 mm/min rate [26] The Young's modulus, the tensile strength, the stress and the strain (elongation) at break were calculated as average values. Three measurements were averaged out to obtain mechanical properties.

The porosity of membranes was calculated in the gravimetric method and can be explained as the volume of the pores divided by the total volume of the membrane. Membranes were dried for 4–5 h at 50°C and weighed with a precision electronic balance to estimate the porosity of the membrane, then infused with kerosene for about 24 h and weighed again after sponging away superficial kerosene with Whatman lint-free filter paper [27]. It is essential to disclose here that kerosene is used instead of water in measuring porosity is because of the lower surface tension which makes it further persistent inside the pores of the membrane [4]. The overall porosity ε_m was calculated using the following equation.

$$\varepsilon_m(\%) = \left[\frac{(w_1 - w_2)/D_k}{(w_1 - w_2)/D_k + \frac{w_2}{D_{\text{pol}}}}\right] \times 100 \quad (1)$$

where w_1 is the weight of the wet membrane; w_2 is the weight of the dry membrane; D_k is the density of kerosene oil (0.82 g/cm^3); (D_{pol}) is the density of polymer: PES = 1.37 g/cm^3.

The porosity of each membrane was measured three times and calculated on average to minimize experimental error.

2.5. Membrane water permeability and BSA rejection

The pure water permeability of the membranes was calculated using a crossflow disc holder, EPDM version 90 mm purchased from Sterlitech, holding the effective membrane area of 50 cm^2. Proceeding to permeability measurements, the membranes were soaked in ultrapure water for 3 h. Membranes were initially compacted at 5 bar transmembrane pressure (TMP) for 1 h. Permeability measurements were conducted at room temperature and at constant cross-flow (1 L/min) and the pressure was varied from 1 to 5 bar. The permeation flux was defined by Eq. (2).

$$J_w = \frac{V}{A \times t} \quad (2)$$

where J_w is the pure water flux (L m^2 h), V is the permeate volume (L), A is the membrane area (m^2) and t the time (h). The rejection of proteins (R) was calculated by the following Eq. (3).

$$R(\%) = 1 - \left(\frac{C_p}{C_f}\right) \times 100 \quad (3).$$

where C_p and C_f are the permeate concentration and the feed concentration, respectively. The concentrations of proteins for both feed and permeate solutions were determined by a UV-Vis spectrophotometer (HACH, DR 5000 spectrophotometer) at 280 nm. It should be illustrated that the permeate was collected at the first 5 min for the rejection study. This experiment was repeated three times to take the average of the result.

2.6. 4-Nitrophenol adsorption

100 mg of PES and hybrid membranes were checked against 100 mL of p-nitrophenol (PNP) stock solutions (0.1 mM). All the PES and hybrid membranes were individually tested against PNP solution. The adsorption capacity of PES and hybrid membranes was monitored by measuring the absorbance using a UV-Vis spectrophotometer.

Table 1
Composition of PES-Ag-SiO_2 hybrid membranes

Membranes	PES (wt.%)	NMP (wt.%)	Ag-SiO_2 (wt.%)
PES	15	85	0.0
PES-Ag-SiO_2-01	15	84.48	0.58
PES-Ag-SiO_2-02	15	83.00	2.00
PES-Ag-SiO_2-03	15	82.66	2.34
PES-Ag-SiO_2-04	15	81.85	3.15
PES-Ag-SiO_2-05	15	80.35	4.65

The decrease in the initial concentration of p-nitrophenols was calculated by the following linear Eq. (4).

Decrease in the initial concentration of

$$p-\text{nitrophenol}=\frac{C_t}{C_0} \tag{4}$$

The membrane's adsorption performance was expressed by adsorption efficiency, A.E. (%), and was calculated using Eq. (5).

$$\text{A.E.}(\%)=\frac{C_0-C_t}{C_t}\times 100=\frac{A_0-A_t}{A_0}\times 100 \tag{5}$$

where C_0 (mg/L) is the initial concentration of NP, C_t (mg/L) is the NP concentration at time t (min), A_0 is the UV-Vis absorption of the original solution and A is the UV-Vis absorption of the same solution at time t (min) in the above equation.

2.7. Antibacterial properties

Antibacterial activity of synthesized hybrid membranes was performed using Gram-negative bacteria *Escherichia coli*. According to JIS L 1902–2002 method [28]. In this method, fresh bacterial test organisms were cultured in a nutrient broth medium and preserved for antimicrobial testing. Further, 25 mL of nutrient broth was prepared in a separate 100 mL conical flask and autoclaved at 121°C with a pressure of 15 psi for 20 min. After autoclaving, cooled at room temperature and inoculate with 50 µL of the previously cultured strain of *E. coli* in a flask. The prepared membranes with different compositions of Ag-SiO_2 were put into each flask. All flasks were incubated at 35°C in an incubator for 18 h. After incubation, optical density (OD) was measured at 600 nm wavelength by using a spectrophotometer [28].

In the disk diffusion method, the bacterial inoculum was homogenously spread by sterile cotton swab on a sterile Petri dish nutrient agar [12]. The pathogenic bacteria used in this study was *Escherichia coli*. Different hybrid membranes (PES-Ag-SiO_2-1 ~ PES-Ag-SiO_2-5) were used to examine its antibacterial activity. For this purpose, three samples from each membrane were cut into 15 mm diameter disk shapes and then transfer to a Petri plate containing a bacterial culture. Then these plates were incubated for 24 h at 36°C ± 1°C, under aerobic conditions. After incubation, confluent bacterial growth was observed.

3. Results and discussions

3.1. Characterization of membranes

3.1.1. Morphology analysis

The cross-sectional morphology of the hybrid membranes was evaluated by FESEM as shown in Fig. 1. It is obvious from the FESEM images that the composite membranes show a similar pattern of morphology. All the prepared membranes exhibited characteristic asymmetric

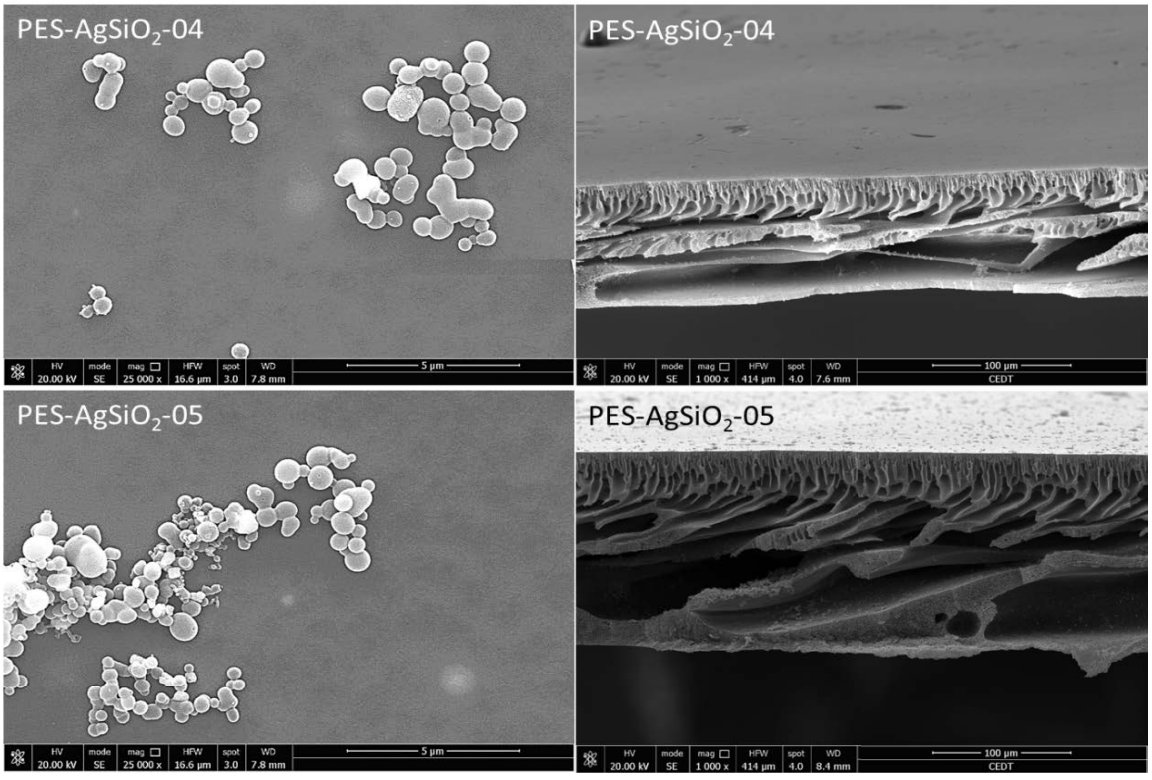

Fig. 1. Surface (left side) and cross-sectional (right side) morphology of membranes.

porous structure of dense top layer followed by fully macro-voids formation at the bottom.

The porosity of all the composite membranes was analyzed and shown in Table 3. The porosity of membranes was increased by adding Ag-SiO_2 NPs. The increase in porosity might be due to enhanced hydrophilicity and macro-voids formation. It can be observed that these nanocomposite membranes possess high porosity varying from 80.12%–84.7% while the pristine membrane has porosity of about 79%. This increase in porosity and macrovoids might reduce the resistance of the membrane and ultimately caused improved pure water flux and may be attributed to the following reasons.

Morphology of the membrane exhibits a vital role in a separation phenomenon, and it is typically determined by the coagulation bath parameters, the viscosity of the dope solution and non-solvent/solvent diffusion rate. Firstly, the thermodynamic stability was decreased by the addition of Ag-SiO_2 NPs in dope solution and hence stimulated the phase separation at a low concentration of polymer, subsequently the formation of more porous structure, high porosity and macrovoids formation [30]. Secondly, incorporation of Ag-SiO_2 NPs delivered more nuclei droplets of the polymer poor phase due to the thermodynamic instability of dope solution and hence responsible for the origination of macrovoids [31]. There could be also a possibility for further development of nuclei together with solvent's diffusional flow and as a result development of macrovoids in PES-Ag-SiO_2 nanocomposite membranes. Thirdly, the rapid mobility of Ag-SiO_2 NPs toward the coagulation bath during the phase separation would decrease interfacial energy among water and the casting film, contributing to enhanced porosity and formation of macrovoids [32].

The scanning electron microscopy (SEM) cross-section images furthermore showed a variation in thickness of the top layer and this could be due to the addition of Ag-SiO_2 NPs. This might be possible due to the variable exchange rate between NMP and water. The surface morphology of hybrid membrane clearly shows Ag-SiO_2 nanoparticles on the surface of membranes while the pure PES membrane shows a clear surface free from nanoparticles.

EDX analysis was carried out for elemental analysis of hybrid membranes. All the membranes showed carbon, oxygen, silica and silver in the elemental compositions as shown in Fig. 2. The accumulation of Ag-SiO_2 is continuously enhanced with the addition of Ag-SiO_2 nanoparticles.

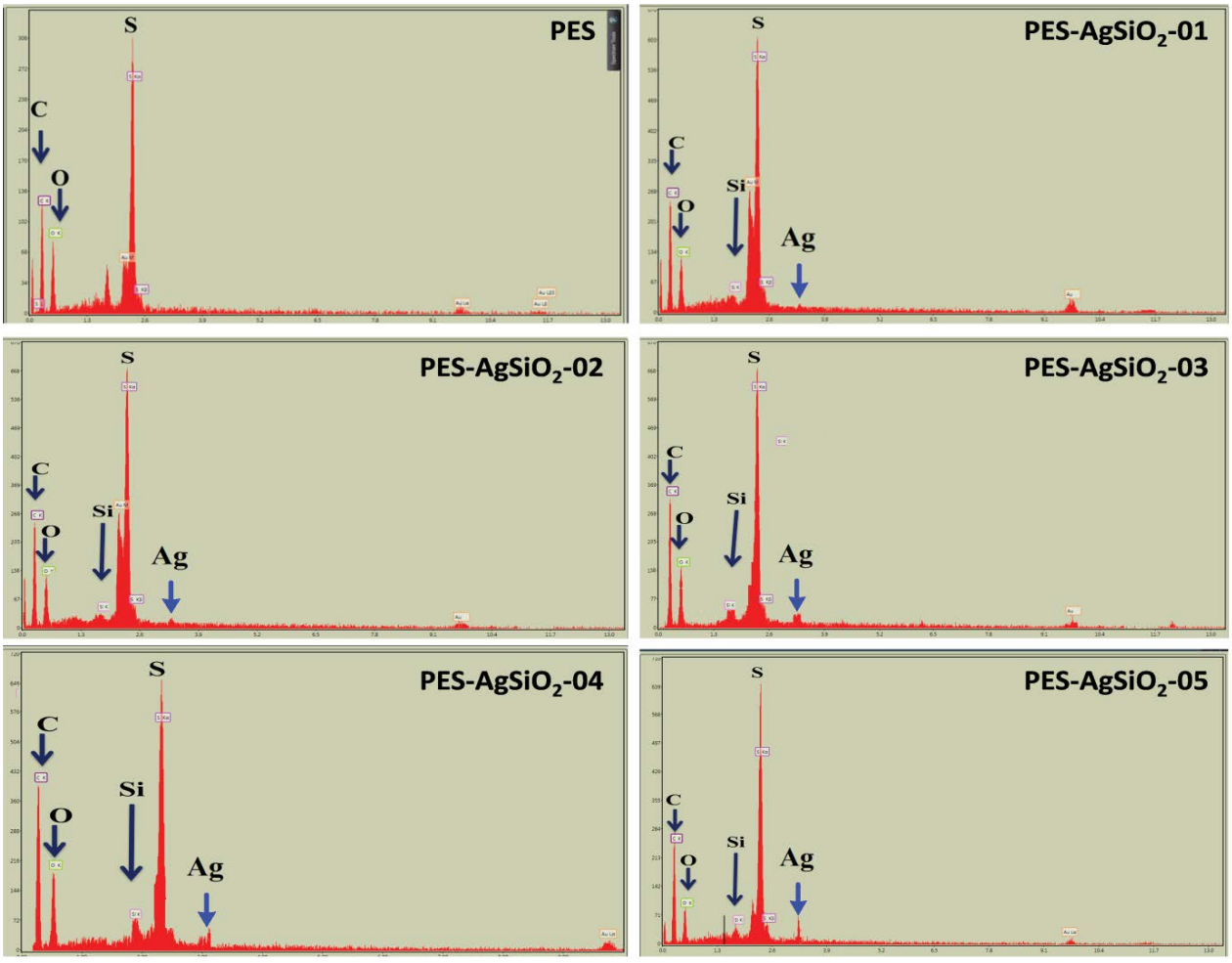

Fig. 2. EDX spectrum of membranes.

3.1.2. X-ray diffraction analysis

X-ray diffraction (XRD) analysis was carried out in order to study the crystallinity of pristine PES as well as Ag-SiO_2 hybrid membrane using wide angle X-ray diffraction (WAXD) (Fig. 3a). The XRD spectrum showed an amorphous halo for all the PES nanocomposite membranes in the range of 15°~30°. The lack of a well crystalline peak and the presence of an amorphous halo suggest the amorphous behavior of PES and hybrid membranes. However, the hybrid membranes with higher contents of Ag-SiO_2 exhibited an additional peak at 44° which might be due to Ag nanoparticles.

3.1.3. Fourier transform infrared spectroscopy analysis

Fourier transform infrared spectroscopy (FT-IR) was analyzed for all the hybrid membranes in order to evaluate the effect of Ag-SiO_2 on the chemical structure of PES (Fig. 3b). FT-IR spectrum of PES revealed absorption bands at 3,470; 2,800–2,900; 1,750; 1,380; 1,233; 1,047 and 886 cm^{-1} which corresponds to O–H, C–H, C=O and C–O stretching vibration [33]. All the hybrid membranes exhibited the same pattern containing the peaks of PES which suggested that the addition of Ag-SiO_2 did not affect the chemical structure of PES.

3.1.4. Contact angle

The contact angle of the Ag-SiO_2 nanocomposite membranes was measured and compared with the pure PES membrane. Pristine PES membrane showed the highest value of contact angle of about 73.4°. The addition of Ag-SiO_2 caused a decrease in contact angle and the results are summarized in Table 2. The decrease in contact angle ultimately increases porosity as well as pure water permeability of the hybrid membranes. The decreasing trend along with the increase in porosity could be observed clearly in Fig. 4a. A similar trend of contact angle was also found in the literature [34]. It is a well-known phenomenon that hydrophilicity is promising for improved pure water flux as well as better antifouling ability [35].

3.1.5. Mechanical properties

Nanocomposite membranes offer a remarkable prospect for improving the mechanical properties of polymers which recognize polymers in utilizing commercial applications [37–41] Addition of nanofillers has played important role in improving the mechanical properties of the polymer [43,44]. On the other hand, porosity also plays an important role in defining the mechanical properties, the higher the porosity value lower the mechanical properties. The porosity of the Ag-SiO_2 nanocomposite membranes increased with the addition of NPs as shown in Table 3 and thus decreasing the tensile properties.

The effect of Ag-SiO_2 on the mechanical properties of Ag-SiO_2-PES hybrid membranes has been evaluated which is shown in Fig. 4b. The mechanical property of hybrid membranes increased with the increase in polymer concentration [45]. Pure PES showed a young modulus of 138.57 N/mm^2. However, the young modulus was gradually decreased by the addition of Ag-SiO_2 due to the imperfect structure caused by the non-uniform dispersion of Ag-SiO_2 nanoparticles in comparison with pure PES. The thickness,

Table 2
Contact angle of PES-Ag-SiO_2 hybrid membranes

Membrane	CA (°)
PES	73.40 ± 0.19
PES-Ag-SiO_2-01	72.67 ± 0.81
PES-Ag-SiO_2-02	71.2 ± 0.91
PES-Ag-SiO_2-03	69.56 ± 0.57
PES-Ag-SiO_2-04	64.88 ± 0.68
PES-Ag-SiO_2-05	58.82 ± 0.72

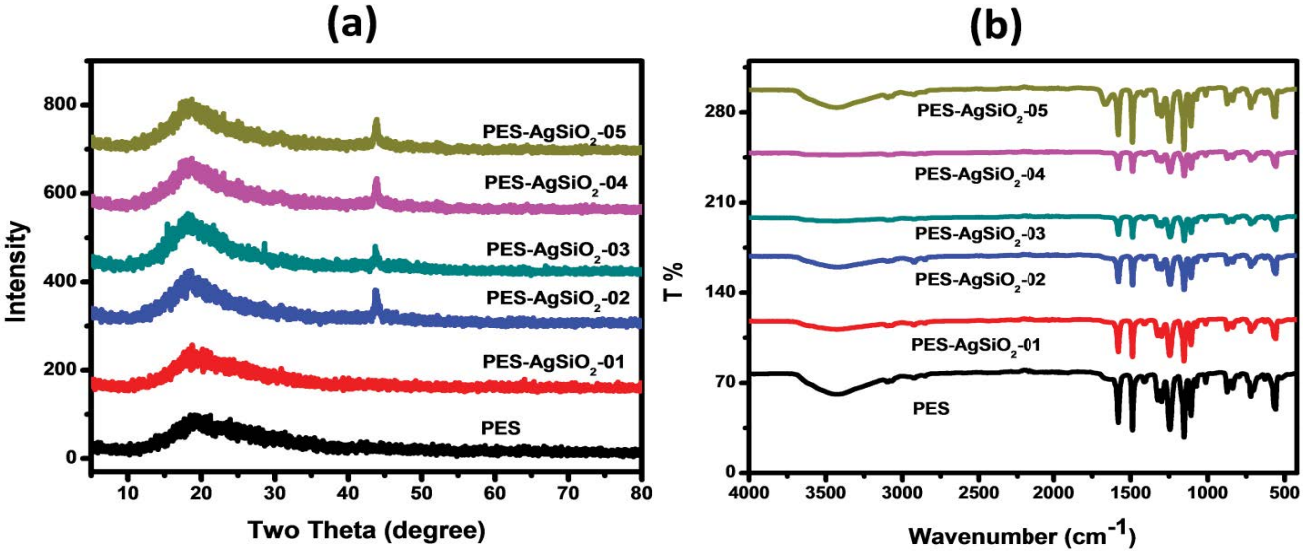

Fig. 3. XRD (a) and FT-IR spectrum (b) of membranes.

tensile stress and young modulus of the PES and hybrid membranes are presented in Table 4.

Table 3
Porosity of PES-Ag-SiO_2 hybrid membranes

Membrane	Porosity (%)
PES	79.00 ± 0.12
PES-Ag-SiO_2-01	80.12 ± 0.40
PES-Ag-SiO_2-02	81.63 ± 1.4
PES-Ag-SiO_2-03	82.97 ± 1.97
PES-Ag-SiO_2-04	83.29 ± 0.95
PES-Ag-SiO_2-05	84.76 ± 1.73

3.1.6. Water permeability

Pure water permeability and filtration are important parameters that should be higher for any promising membrane. The increase in the steady-state flux behavior of the nanocomposite membranes with the addition of Ag-SiO_2 can be interpreted in many ways. First of all, the increase in hydrophilicity could increase the affinity of water molecules inside the polymer matrix of the membranes, then ultimately improved the water permeability. Secondly, interfacial cavities between the PES polymer matrix and Ag-SiO_2 nanoparticles find an additional water passage to enhance water permeability under transmembrane pressure. In addition, by incorporation of Ag-SiO_2 nanoparticle provide additional polymer free volume and hence increased the pure water flux. The same behavior was found by the

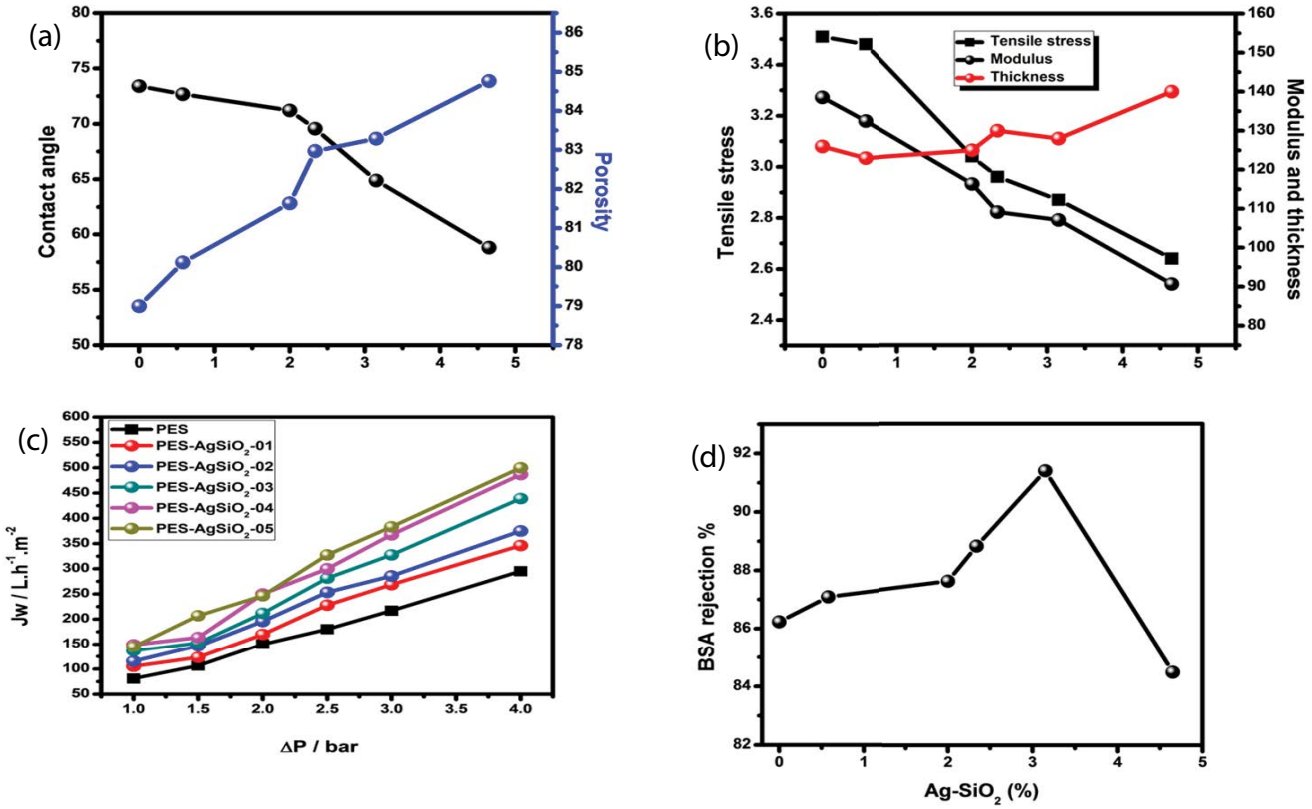

Fig. 4. Contact angle and porosity of membranes (a), tensile strength, modulus and thickness of membranes (b), water flux of hybrid membranes (c), and bovine serum albumin protein (BSA) rejection of membranes (d).

Table 4
Mechanical properties of PES-Ag-SiO_2 hybrid membranes

PES membrane	Film thickness (μm)	Tensile stress at maximum load (N/mm^2)	Modulus Emod [(N/mm^2)]
PES	126 ± 1	3.51	138.57
PES-Ag-SiO_2-01	123 ± 2	3.48	132.54
PES-Ag-SiO_2-02	125 ± 2	3.04	116.32
PES-Ag-SiO_2-03	130 ± 3	2.96	109.14
PES-Ag-SiO_2-04	128 ± 4	2.87	107.14
PES-Ag-SiO_2-05	140 ± 3	2.64	90.69

addition of ZnO nanoparticles in a recent study by Li et al. [46]. The water flux and filtration behavior of pure PES and prepared hybrid membranes (PES-Ag-SiO_2-1 ~ PES-Ag-SiO_2-5) are depicted in Fig. 4c. Here it clearly shows that water flux increased with different amount of NPs in the polymer matrix [47]. Assuming that the pure PES membrane and PES-Ag-SiO_2 membranes have similar surface pore sizes, the increase in water flux may be due to the addition of the Ag-SiO_2. PES-Ag-SiO_2-5 has higher Ag-SiO_2 contents and thus had higher water flux as compared to other hybrid membranes. The results of improved pure water flux could also be related to the morphology of the nanocomposite membranes. The formation of macrovoids resulted in an increase in water permeability as confirmed by the SEM images in the previous section and Fig. 1. The results of water permeability are summarized in Table 5.

3.1.7. BSA rejection

The performance of the ultrafiltration nanocomposite membranes was performed using bovine serum albumin (BSA) as model foulant. Fig. 4d shows that the incorporation of the Ag-SiO_2 NPs improved the membrane surface hydrophilicity and decreased BSA adsorption. It can be observed that modified membranes adsorb less protein with Ag-SiO_2-4 showing the least BSA adsorption and have the maximum rejection of 91.3%. The. The decrease in BSA rejection was mainly attributed to the increasing pore size and the higher porosity (PES-Ag-SiO_2-05). This could also be explained that the addition of a different amount of NPs might modify the properties of the membrane surface. The other reason for the decrease in BSA rejection could also be due to the aggregation of Ag-SiO_2 in our case for membrane 5 and this could also be confirmed with the SEM images. One of the main factors influencing the increasing the protein fouling is the hydrophobic–hydrophobic interaction among membrane surface and the protein molecules. Therefore the phenomenon of hydrophobic interaction can be reduced by modification of the membrane, to make membrane surface hydrophilic, either by the incorporation of nanomaterials or by the addition of some other hydrophilic additives. Once the surface became hydrophilic, there is less chance of protein molecules to adsorb on the surface of the membrane and as a result, improved protein fouling resistance [48,49]. Wang and Tang [50] described the mechanism of BSA fouling and they established that protein fouling is generally dependent on the properties of the membranes. They revealed that smooth, hydrophilic and negatively charged membranes exhibited low flux drop at the early fouling stage. Subsequently, the properties of the membranes, particularly hydrophobic/hydrophilic characteristics could perform a significant role in the protein fouling mechanism. The BSA rejection results are shown in Fig. 4d.

Table 5
Pure water permeability of PES-Ag-SiO_2 hybrid membranes

Membrane	Water permeability	
	L_p (L/h/m^2 bar)	R^2
PES-virgin	73.30	0.99
PES-Ag-SiO_2-1	88.05	0.98
PES-Ag-SiO_2-02	96.55	0.98
PES-Ag-SiO_2-03	109.8	0.98
PES-Ag-SiO_2-04	121.8	0.98
PES-Ag-SiO_2-05	127.7	0.99

3.1.8. Adsorption of p-nitrophenol

Removal of Organic pollutant is extremely important from the effluents because of their toxic, carcinogenic and mutagenic nature [24, 29, 36, 42]. PES hybrid membranes were examined for p-nitrophenol adsorption. The adsorption properties of all hybrid membranes were also compared with pure PES polymer for p-nitrophenol adsorption as shown in Fig. 5. 100 mg of each hybrid membrane and pure PES were used for the adsorption of 100 mL of p-nitrophenol solution. The result indicates that PES-Ag-SiO_2-5 showed good adsorption performance for the p-nitrophenol analyte. The concentration of the p-nitrophenol was gradually decreased in effluent with time as shown in Fig. 5a. PES-Ag-SiO_2-5 showed a good adsorption performance which almost adsorbed 26.8 of p-nitrophenol

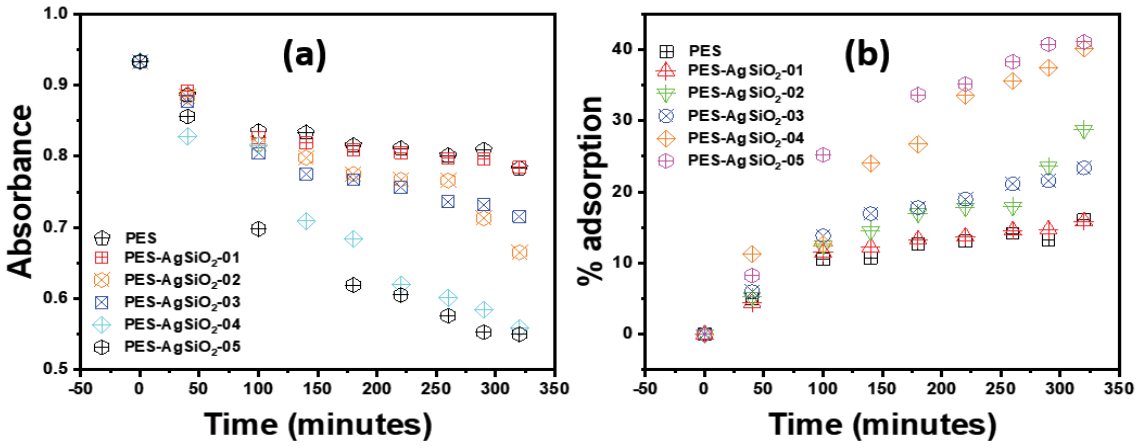

Fig. 5. Linear plot based on C_t/C_0 (a), and % adsorption of p-nitrophenol by PES and its hybrid membranes (b).

within 3 h. However, after 5.3 h the adsorption capacity was increased to 40.0%. Similarly, after 24 h the adsorption capacity was further enhanced to 56.8% for PES-Ag-SiO_2-5. It means that the nanocomposite PES-Ag-SiO_2-5 removed 56.8% of highly toxic organic p-nitrophenol pollutants from wastewater. The percent removal of p-nitrophenol is shown in Fig. 5b. After 24 h the highest percent adsorption for p-nitrophenol was shown by PES-Ag-SiO_2-5.

3.2. Antibacterial activity

The zone inhibition method indicates the bacterial growth retardation or inhibition due to the diffusion of materials and metal ions into the growing medium on an agar plate. Fig. 6a indicates the control membrane without any nanomaterial involvement in the fabrication of membrane showed here without any significant zone of inhibition. While membrane fabrication with nanomaterials up to 5% zone of inhibition of bacterial growth was increasing significantly. In our study, a 15 mm zone of inhibition size was observed of 1 cm diameter of the composite membrane which is clearly shown in Fig. 6. In previous studies, composite membrane antimicrobial activity was reported on solid nutrient agar medium. Further, increasing the concentration of nanomaterials in the nanocomposite membrane, proportionally increase the growth retardation and decease the optical density. Composite membrane with 6% silver nanomaterial, when incubated with *E. coli* culture and *P. peli* culture then turbidity decrease up to 77.78% and 76.30% in liquid medium. Sherman et al. [30] have been observed improved anti-biofouling and antibacterial membrane property when its fabrication modified by amendment of Ag-SiO_2. Similarly, in other reports, Zhang et al. [51] amended biogenic silver nanoparticles in polyethersulfone membrane preparation and further studied anti-biofouling and anti-biofilm formation properties of these nanocomposite membranes.

4. Conclusion

In conclusion, this study proved the feasibility of producing PES-Ag-SiO_2 hybrid membranes with a finger-like

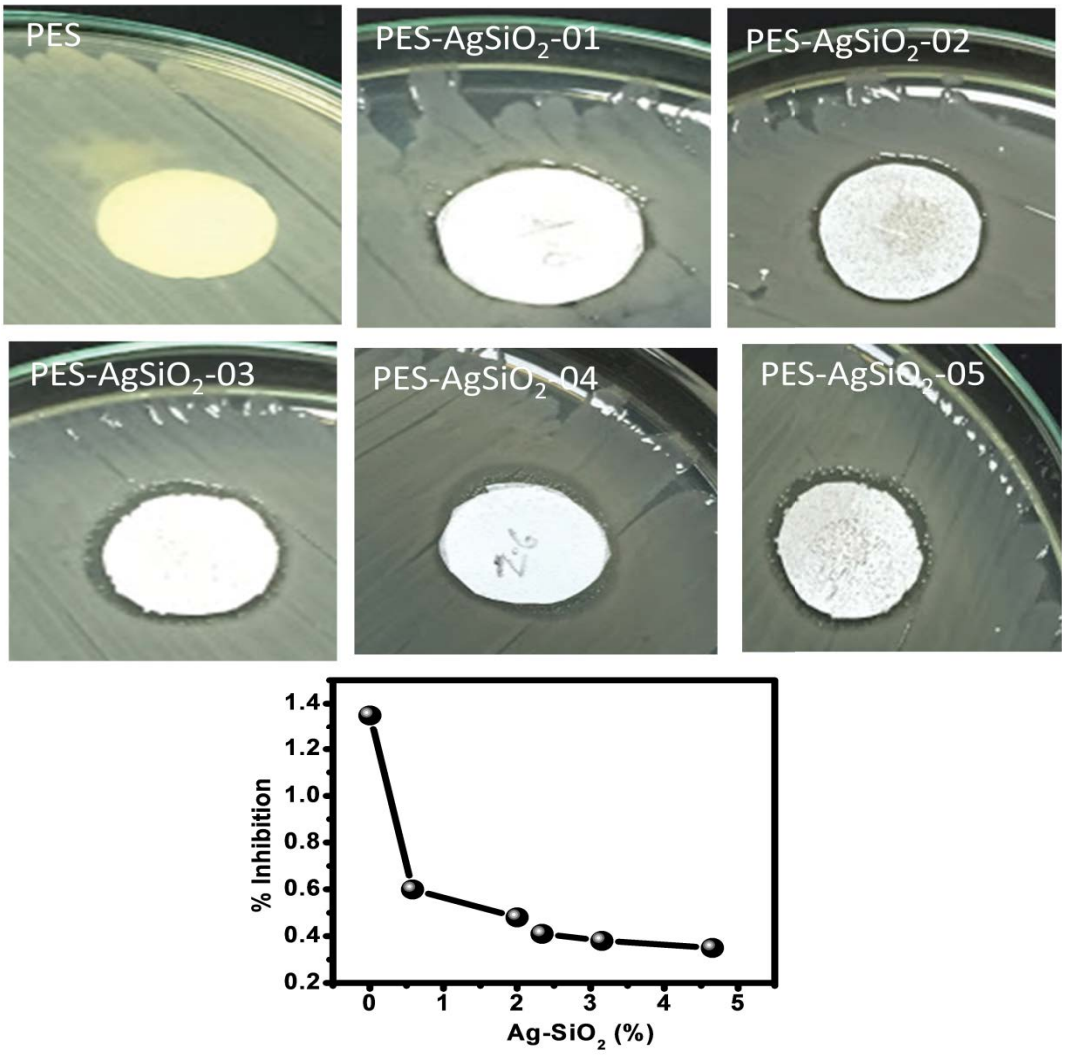

Fig. 6. Anti-bacterial activity of membranes.

structure and porous sublayer. The addition of Ag-SiO_2 caused an increase in hydrophilicity by decreasing the contact angle. The hybrid membranes showed lower mechanical properties because of porosity produced in the membranes by the addition of Ag-SiO_2. Additionally, the addition of Ag-SiO_2 also affected the water permeability of the PES membrane. Hybrid membranes showed higher water flux as compared to the pristine PES membrane. The hybrid membranes exhibited an improved BSA rejection, nitrophenol adsorption and antibacterial properties as compared to the pristine PES membrane. The SiO_2 impregnated membranes could be suitable for pretreatment as ultrafiltration. All the fabricated nanocomposite membranes exhibit excellent antibacterial activity, showing that Ag-SiO_2 nanoparticle embedded PES membranes could be effective anti-biofouling membranes.

Acknowledgments

This paper is funded by Taif University Researchers Supporting Project number (TURSP-2020/90), Taif University, Taif, Saudi Arabia. Therefore, the authors would like to thank Taif University for this financial support. This Deanship of Scientific Research (DSR), at King Abdulaziz University, Jeddah, Saudi Arabia has funded this project under grant no. (KEP- 31-130-42).

References

[1] A.K. Singla, M. Chawla, Chitosan: some pharmaceutical and biological aspects — an update, J. Pharm. Pharmacol., 53 (2001) 1047–1067.
[2] M. Rinaudo, Chitin and chitosan: properties and applications, Prog. Polym. Sci., 31 (2006) 603–632.
[3] M.N.R. Kumar, A review of chitin and chitosan applications, React. Funct. Polym., 46 (2000) 1–27.
[4] Q.F. Alsalhy, H.A. Salih, S. Simone, M. Zablouk, E. Drioli, A. Figoli, Poly(ether sulfone) (PES) hollow-fiber membranes prepared from various spinning parameters, Desalination, 345 (2014) 21–35.
[5] Y. Zhang, X. Yu, S. Gong, C. Ye, Z. Fan, H. Lin, Antibiofilm activity of *Bacillus pumilus* SW9 against initial biofouling on microfiltration membranes, Appl. Microbiol. Biotechnol., 98 (2014) 1309–1320.
[6] M. Zhang, K. Zhang, B. De Gusseme, W. Verstraete, Biogenic silver nanoparticles (bio-Ag^0) decrease biofouling of bio-Ag^0/PES nanocomposite membranes, Water Res., 46 (2012) 2077–2087.
[7] O. Choi, K.K. Deng, N.-J. Kim, L. Ross, R.Y. Surampalli, Z. Hu, The inhibitory effects of silver nanoparticles, silver ions, and silver chloride colloids on microbial growth, Water Res., 42 (2008) 3066–3074.
[8] D. Rana, T. Matsuura, Surface modifications for antifouling membranes, Chem. Rev., 110 (2010) 2448–2471.
[9] S. Kappachery, D. Paul, J. Yoon, J.H. Kweon, Vanillin, a potential agent to prevent biofouling of reverse osmosis membrane, Biofouling, 26 (2010) 667–672.
[10] N. Hilal, V. Kochkodan, L. Al-Khatib, T. Levadna, Surface modified polymeric membranes to reduce (bio) fouling: a microbiological study using *E. coli*, Desalination, 167 (2004) 293–300.
[11] H.-L. Yang, J. Chun-Te Lin, C. Huang, Application of nanosilver surface modification to RO membrane and spacer for mitigating biofouling in seawater desalination, Water Res., 43 (2009) 3777–3786.
[12] X. Cao, M. Tang, F. Liu, Y. Nie, C. Zhao, Immobilization of silver nanoparticles onto sulfonated polyethersulfone membranes as antibacterial materials, Colloids Surf., B, 81 (2010) 555–562.
[13] D.S. Wavhal, E.R. Fisher, Hydrophilic modification of polyethersulfone membranes by low temperature plasma-induced graft polymerization, J. Membr. Sci., 209 (2002) 255–269.
[14] M.N. Abu Seman, D. Johnson, S. Al-Malek, N. Hilal, Surface modification of nanofiltration membrane for reduction of membrane fouling, Desal. Water Treat., 10 (2009) 298–305.
[15] W. Zhao, J. Huang, B. Fang, S. Nie, N. Yi, B. Su, H. Li, C. Zhao, Modification of polyethersulfone membrane by blending semi-interpenetrating network polymeric nanoparticles, J. Membr. Sci., 369 (2011) 258–266.
[16] Y. Zhang, J. Guo, G. Han, Y. Bai, Q. Ge, J. Ma, C.H. Lau, L. Shao, Molecularly soldered covalent organic frameworks for ultrafast precision sieving, Sci. Adv., 7 (2021) eabe8706, doi: 10.1126/sciadv.abe8706.
[17] M. Amin, A. Alazba, U. Manzoor, A review of removal of pollutants from water/wastewater using different types of nanomaterials, Adv. Mater. Sci. Eng., 2014 (2014) 1–24.
[18] R.L. Davies, S.F. Etris, The development and functions of silver in water purification and disease control, Catal. Today, 36 (1997) 107–114.
[19] Q. Feng, J. Wu, G. Chen, F. Cui, T. Kim, J. Kim, A mechanistic study of the antibacterial effect of silver ions on *Escherichia coli* and *Staphylococcus aureus*, J. Biomed. Mater. Res., 52 (2000) 662–668.
[20] I. Sondi, B. Salopek-Sondi, Silver nanoparticles as antimicrobial agent: a case study on *E. coli* as a model for Gram-negative bacteria, J. Colloid Interface Sci., 275 (2004) 177–182.
[21] V. Alt, T. Bechert, P. Steinrücke, M. Wagener, P. Seidel, E. Dingeldein, E. Domann, R. Schnettler, An in vitro assessment of the antibacterial properties and cytotoxicity of nanoparticulate silver bone cement, Biomaterials, 25 (2004) 4383–4391.
[22] N. Daneshvar, M. Behnajady, Y.Z. Asghar, Photooxidative degradation of 4-Nitrophenol (4-NP) in UV/H_2O_2 process: influence of operational parameters and reaction mechanism, J. Hazard. Mater., 139 (2007) 275–279.
[23] Z.I. Bhatti, H. Toda, K. Furukawa, p-nitrophenol degradation by activated sludge attached on nonwovens, Water Res., 36 (2002) 1135–1142.
[24] Y. Shi, X.-L. Zhang, G. Feng, X. Chen, Z.-H. Lu, Ag–SiO_2 nanocomposites with plum-pudding structure as catalyst for hydrogenation of 4-Nitrophenol, Ceram. Int., 41 (2015) 14660–14667.
[25] S.A. Khan, S.B. Khan, A.M. Asiri, Core–shell cobalt oxide mesoporous silica based efficient electro-catalyst for oxygen evolution, New J. Chem., 39 (2015) 5561–5569.
[26] B. Qian, J. Li, Q. Wei, P. Bai, B. Fang, C. Zhao, Preparation and characterization of pH-sensitive polyethersulfone hollow fiber membrane for flux control, J. Membr. Sci., 344 (2009) 297–303.
[27] D. Wang, Q. Wei, Y. Zhang, C. Zhao, Molecularly imprinted polyethersulfone microfibers for the binding and recognition of bisphenol A, J. Appl. Poly. Sci., 114 (2009) 4036–4041.
[28] K. Yang, Z. Liu, M. Mao, X. Zhang, C. Zhao, N. Nishi, Molecularly imprinted polyethersulfone microspheres for the binding and recognition of bisphenol A, Anal. Chim. Acta, 546 (2005) 30–36.
[29] W.L. Chou, D.G. Yu, M.C. Yang, The preparation and characterization of silver-loading cellulose acetate hollow fiber membrane for water treatment, Polym. Adv. Technol., 16 (2005) 600–607.
[30] J.G. Cappuccino, N. Sherman, Microbiology: A Laboratory Manual, Pearson/Benjamin Cummings, 2008.
[31] Y.-n. Yang, W. Jun, Z. Qing-zhu, C. Xue-si, Z. Hui-xuan, The research of rheology and thermodynamics of organic–inorganic hybrid membrane during the membrane formation, J. Membr. Sci., 311 (2008) 200–207.
[32] C.A. Smolders, A.J. Reuvers, R.M. Boom, I.M. Wienk, Microstructures in phase-inversion membranes. Part 1. Formation of macrovoids, J. Membr. Sci., 73 (1992) 259–275.
[33] Z. Fan, Z. Wang, N. Sun, J. Wang, S. Wang, Performance improvement of polysulfone ultrafiltration membrane by blending with polyaniline nanofibers, J. Membr. Sci., 320 (2008) 363–371.

[34] R.J. Gohari, E. Halakoo, N. Nazri, W.J. Lau, T. Matsuura, A.F. Ismail, Improving performance and antifouling capability of PES UF membranes via blending with highly hydrophilic hydrous manganese dioxide nanoparticles, Desalination, 335 (2014) 87–95.
[35] E. Saljoughi, T. Mohammadi, Cellulose acetate (CA)/ polyvinylpyrrolidone (PVP) blend asymmetric membranes: preparation, morphology and performance, Desalination, 249 (2009) 850–854.
[36] L. Shen, X. Bian, X. Lu, L. Shi, Z. Liu, L. Chen, Z. Hou, K. Fan, Preparation and characterization of ZnO/polyethersulfone (PES) hybrid membranes, Desalination, 293 (2012) 21–29.
[37] E.S. Jang, S.B. Khan, J. Seo, K. Akhtar, J. Choi, K.I. Kim, H. Han, Synthesis and characterization of novel UV-curable PU-Si hybrids: influence of silica on thermal, mechanical, and water sorption properties of polyurethane acrylates, Macromol. Res., 19 (2011) 1006–1013.
[38] S.B. Khan, J.-W. Lee, H.M. Marwani, K. Akhtar, A.M. Asiri, J. Seo, A.A.P. Khan, H. Han, Polybenzimidazole hybrid membranes as a selective adsorbent of mercury, Composites, Part B, 56 (2014) 392–396.
[39] D. Kim, M. Jang, J. Seo, K.-H. Nam, H. Han, S.B. Khan, UV-cured poly (urethane acrylate) composite films containing surface-modified tetrapod ZnO whiskers, Compos. Sci. Technol., 75 (2013) 84–92.
[40] D. Kim, Y. Lee, J. Seo, H. Han, S.B. Khan, Preparation and properties of poly(urethane acrylate)(PUA) and tetrapod ZnO whisker (TZnO-W) composite films, Polym. Int., 62 (2013) 257–265.
[41] J. Seo, G. Jeon, E.S. Jang, S. Bahadar Khan, H. Han, Preparation and properties of poly (propylene carbonate) and nanosized ZnO composite films for packaging applications, J. Appl. Polym. Sci., 122 (2011) 1101–1108.
[42] Y. Lee, D. Kim, J. Seo, H. Han, S.B. Khan, CuO embedded chitosan spheres as antibacterial adsorbent for dyes, Polym. Int., 62 (2013) 1386–1394.
[43] M. Lim, H. Kwon, D. Kim, J. Seo, H. Han, S.B. Khan, Highly-enhanced water resistant and oxygen barrier properties of cross-linked poly (vinyl alcohol) hybrid films for packaging applications, Prog. Org. Coat., 85 (2015) 68–75.
[44] K.-H. Nam, K. Seo, J. Seo, S.B. Khan, H. Han, Ultraviolet-curable polyurethane acrylate nanocomposite coatings based on surface-modified calcium carbonate, Prog. Org. Coat., 85 (2015) 22–30.
[45] J.-N. Shen, H.-M. Ruan, L.-G. Wu, C.-J. Gao, Preparation and characterization of PEG-g-MWCNTs/PSf nano-hybrid membranes with hydrophilicity and antifouling properties, Chem. Eng. J., 168 (2011) 1272–1278.
[46] X. Li, J. Li, B.V.D. Bruggen, X. Sun, J. Shen, W. Han, L. Wang, Fouling behavior of polyethersulfone ultrafiltration membranes functionalized with sol–gel formed ZnO nanoparticles, RSC Adv., 5 (2015) 50711–50719.
[47] S.B. Khan, K.A. Alamry, E.N. Bifari, A.M. Asiri, M. Yasir, L. Gzara, R.Z. Ahmad, Assessment of antibacterial cellulose nanocomposites for water permeability and salt rejection, J. Ind. Eng. Chem., 24 (2015) 266–275.
[48] K.S. Kim, K.H. Lee, K. Cho, C.E. Park, Surface modification of polysulfone ultrafiltration membrane by oxygen plasma treatment, J. Membr. Sci., 199 (2002) 135–145.
[49] D.Y. Koseoglu-Imer, B. Kose, M. Altinbas, I. Koyuncu, The production of polysulfone (PS) membrane with silver nanoparticles (AgNP): physical properties, filtration performances, and biofouling resistances of membranes, J. Membr. Sci., 428 (2013) 620–628.
[50] Y.-N. Wang, C.Y. Tang, Protein fouling of nanofiltration, reverse osmosis, and ultrafiltration membranes—the role of hydrodynamic conditions, solution chemistry, and membrane properties, J. Membr. Sci., 376 (2011) 275–282.
[51] Y. Zhao, Y. Zhang, F. Li, Y. Bai, Y. Pan, J. Ma, S. Zhang, L. Shao, Ultra-robust superwetting hierarchical membranes constructed by coordination complex networks for oily water treatment, J. Membr. Sci., 627 (2021) 119234, doi: 10.1016/j.memsci.2021.119234.